

Full Paper

A Perturbation Method for the 3D Finite Element Modeling of Electrostatically Driven MEMS

Mohamed Boutaayamou^{1,*}, Ruth V. Sabariego¹ and Patrick Dular^{1,2}

¹ Department of Electrical Engineering and Computer Science, Applied and Computational Electromagnetics (ACE), ¹ University of Liège, ^{1,2} FNRS

Sart Tilman Campus, Building B28, B-4000, Liège, Belgium

E-mails: MBoutaayamou@ulg.ac.be; R.Sabariego@ulg.ac.be; Patrick.Dular@ulg.ac.be

* Author to whom correspondence should be addressed.

Received: 14 September 2007 / Accepted: 8 February 2008 / Published: 19 February 2008

Abstract: In this paper, a finite element (FE) procedure for modeling electrostatically actuated MEMS is presented. It concerns a perturbation method for computing electrostatic field distortions due to moving conductors. The computation is split in two steps. First, an unperturbed problem (in the absence of certain conductors) is solved with the conventional FE method in the complete domain. Second, a perturbation problem is solved in a reduced region with an additional conductor using the solution of the unperturbed problem as a source. When the perturbing region is close to the original source field, an iterative computation may be required. The developed procedure offers the advantage of solving sub-problems in reduced domains and consequently of benefiting from different problem-adapted meshes. This approach allows for computational efficiency by decreasing the size of the problem.

Keywords: Electrostatic field distortions, finite element method, perturbation method, MEMS.

1. Introduction

Increased functionality of MEMS has led to the development of micro-structures that are more and more complex. Besides, modeling tools have not kept the pace with this growth. Indeed, the simulation of a device allows to optimize its design, to improve its performance, and to minimize development time and cost by avoiding unnecessary design cycles and foundry runs. To achieve these objectives, the

development of new and more efficient modeling techniques adapted to the requirements of MEMS, has to be carried out [1].

Several numerical methods have been proposed for the simulation of MEMS. Lumped or reduced order models and semi-analytical methods [2][3] allow to predict the behaviour of simple micro-structures. However they are no longer applicable for devices, such as comb drives, electrostatic motors or deflectable 3D micromirrors, where fringing electrostatic fields are dominant [4][5][6]. The FE method can accurately compute these fringing effects at the expense of a dense discretization near the corners of the device [7]. Further the FE modeling of MEMS accounting for their movement needs a completely new mesh and computation for each new position what is specially expensive when dealing with 3D models.

The scope of this work is to introduce a perturbation method for the FE modeling of electrostatically actuated MEMS. An unperturbed problem is first solved in a large mesh taking advantage of any symmetry and excluding additional regions and thus avoiding their mesh. Its solution is applied as a source to the further computations of the perturbed problems when conductive regions are added [8][9][10]. It benefits from the use of different subproblem-adapted meshes, this way the computational efficiency increases as the size of each sub-problem diminishes [9]. For some positions where the coupling between regions is significant, an iterative procedure is required to ensure an accurate solution. Successive perturbations in each region are thus calculated not only from the original source region to the added conductor but also from the latter to the former. A global-to-local method for static electric field calculations is presented in [11]. Herein, the mesh of the local domain is included in the one of the global domain, whereas in the proposed perturbation method, the meshes of the perturbing regions are independent of the meshes of the unperturbed domain, which is a clear advantage with respect to the classical FE approach.

As test case, we consider a micro-beam subjected to an electrostatic field created by a micro-capacitor. The micro-beam is meshed independently of the complete domain between the two electrodes of the device. The electrostatic field is computed in the vicinity of the corners of the micro-beam by means of the perturbation method. For the sake of validation, results are compared to those calculated by the conventional FE approach. Furthermore, the accuracy of the perturbation method is discussed as a function of the extension of the reduced domain.

2. Electric Scalar Potential Weak Formulation

We consider an electrostatic problem in a domain Ω , with boundary $\partial\Omega$, of the 2-D or 3-D Euclidean space. The conductive parts of Ω are denoted Ω_c . The governing differential equations and constitutive law of the electrostatic problem in Ω are [12]

$$\mathbf{curl} \mathbf{e} = 0, \quad \mathbf{div} \mathbf{d} = q, \quad \mathbf{d} = \varepsilon \mathbf{e}, \quad (1a-b-c)$$

where \mathbf{e} is the electric field, \mathbf{d} is the electric flux density, q is the electric charge density and ε is the electric permittivity (symbols in bold are vectors). In charge free regions, we obtain from (1a-b-c) the following equation in terms of the electric scalar potential v [12]

$$\mathbf{div}(-\varepsilon \mathbf{grad} v) = 0. \quad (2)$$

The electrostatic problem can be calculated as a solution of the electric scalar potential formulation obtained from the weak form of the Laplace equation (2) as [13]

$$(-\varepsilon \mathbf{grad} v, \mathbf{grad} v')_{\Omega} - \langle \mathbf{n} \cdot \mathbf{d}, v' \rangle_{\Gamma_d} = 0, \quad \forall v' \in F(\Omega), \quad (3)$$

where $F(\Omega)$ is the function space defined on Ω containing the basis functions for v as well as for the test function v' ; $(\cdot, \cdot)_{\Omega}$ and $\langle \cdot, \cdot \rangle_{\Gamma_d}$ respectively denote a volume integral in Ω and a surface integral on Γ of products of scalar or vector fields. The surface integral term in (3) is used for fixing a natural boundary condition (usually homogeneous for a tangent field constraint) on a portion Γ of the boundary of Ω ; \mathbf{n} is the unit normal exterior to Ω .

3. Perturbation Method

Hereafter, the subscripts u and p refer to the unperturbed and perturbed quantities and associated domains, respectively. An unperturbed problem is first defined in Ω without considering the properties of a so-called perturbing region $\Omega_{c,p}$ which will further lead to field distortions [8][9][10]. At the discrete level, this region is not described in the mesh of Ω . The perturbation problem focuses thus on $\Omega_{c,p}$ and its neighborhood, their union Ω_p being adequately defined and meshed will serve as the studied domain. Electric field distortions appear when a perturbing conductive region $\Omega_{c,p}$ is added to the initial configuration. The perturbation problem is defined as an electrostatic problem in Ω_p .

Particularizing (1a-b-c) for both the unperturbed and perturbed problems, we obtain [8]

$$\mathbf{curl} \mathbf{e}_u = 0, \quad \text{div} \mathbf{d}_u = 0, \quad \mathbf{d}_u = \varepsilon_u \mathbf{e}_u, \quad (4a-b-c)$$

$$\mathbf{curl} \mathbf{e}_p = 0, \quad \text{div} \mathbf{d}_p = 0, \quad \mathbf{d}_p = \varepsilon_p \mathbf{e}_p. \quad (5a-b-c)$$

Equations (4b) and (5b) assume that no charge density exists in the considered regions. Subtracting the unperturbed equations from the perturbed ones, one gets [8]

$$\mathbf{curl} \mathbf{e} = 0, \quad \text{div} \mathbf{d} = 0, \quad \mathbf{d} = \varepsilon_p \mathbf{e} + (\varepsilon_p - \varepsilon_u) \mathbf{e}_u, \quad (6a-b-c)$$

with the field perturbations [8]: $\mathbf{e} = \mathbf{e}_p - \mathbf{e}_u$ and $\mathbf{d} = \mathbf{d}_p - \mathbf{d}_u$. Note that if $\varepsilon_p \neq \varepsilon_u$, an additional source term given by the unperturbed solution $(\varepsilon_p - \varepsilon_u) \mathbf{e}_u$ is considered in (6c). For the sake of simplicity, ε_p and ε_u are kept equal.

For added perfect conductors, carrying floating potentials, one must have $\mathbf{n} \times \mathbf{e}_p |_{\partial\Omega_{c,p}} = 0$ and consequently $\mathbf{n} \times \mathbf{e} |_{\partial\Omega_{c,p}} = -\mathbf{n} \times \mathbf{e}_u |_{\partial\Omega_{c,p}}$. This leads to the following condition on the perturbation electric scalar potential

$$v = -v_u |_{\partial\Omega_{c,p}}. \quad (7)$$

This way, v_u acts as a source for the perturbation problem.

Two independent meshes are used. A mesh of the whole domain without any additional conductive regions and a mesh of the perturbing regions. A projection of the results between one mesh and the other is then required.

3.1. Unperturbed electric scalar potential formulation

Particularizing ($v = v_u$) and solving (3), the unperturbed problem is given by

$$(-\varepsilon \mathbf{grad} v_u, \mathbf{grad} v')_{\Omega} - \langle \mathbf{n} \cdot \mathbf{d}_u, v' \rangle_{\Gamma_d} = 0, \quad \forall v' \in F(\Omega). \quad (8)$$

3.2. Perturbation electric scalar potential formulation

The source of the perturbation problem, v_s , is determined in the new added perturbing conductive region $\Omega_{c,p}$ through a projection method [14]. Given the conductive nature of the perturbing region, the projection of v_u from its original mesh to that of $\Omega_{c,p}$ is limited to $\partial\Omega_{c,p}$. It reads

$$\langle \mathbf{grad} v_s, \mathbf{grad} v' \rangle_{\partial\Omega_{c,p}} - \langle \mathbf{grad} v_u, \mathbf{grad} v' \rangle_{\partial\Omega_{c,p}} = 0, \quad \forall v' \in F(\partial\Omega_{c,p}), \quad (9)$$

where the function space $F(\partial\Omega_{c,p})$ contains v_s and its associated test function v' . At the discrete level, v_s is discretized with nodal FEs and is associated to a gauge condition by fixing a nodal value in $\partial\Omega_{c,p}$.

In case of a dielectric perturbing region, the projection should be extended to the whole domain $\Omega_{c,p}$. Besides, we choose to directly project $\mathbf{grad} v_u$ in order to ensure a better numerical behaviour in the ensuing equations where the involved quantities are also gradients.

The perturbation problem is completely characterised by (3) applied to the perturbation potential v as follows

$$(-\varepsilon \mathbf{grad} v, \mathbf{grad} v')_{\Omega_p} - \langle \mathbf{n} \cdot \mathbf{d}, v' \rangle_{\Gamma_{dp}} = 0, \quad \forall v' \in F(\Omega_p), \quad (10)$$

with a Dirichlet boundary condition defined as $v = -v_s |_{\partial\Omega_{c,p}}$.

For a micro-beam subjected to a floating potential and placed inside a parallel-plate capacitor (Fig. 1), the processes of the resolution and projection of the electric scalar potential from one mesh to the other are represented in Fig. 2. The domain Ω surrounding the micro-beam is coarsely meshed while the domain Ω_p containing the micro structure has an adapted mesh especially fine in the vicinity of the corners.

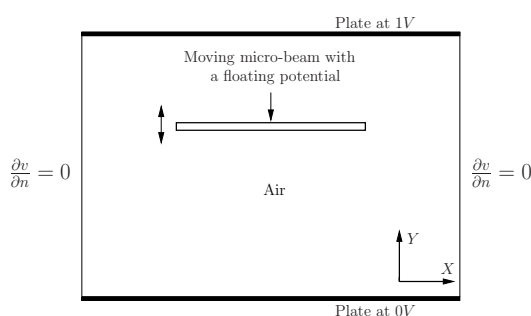


Figure 1. A moving micro-beam carrying a floating potential inside a parallel-plate capacitor

4. Iterative Sequence of Perturbation Electric Scalar Potential Problems

When the perturbing region $\Omega_{c,p}$ is close to the original source field, an iterative sequence has to be carried out. Each region gives a suitable correction as a perturbation with an accuracy dependent of the fineness of its mesh.

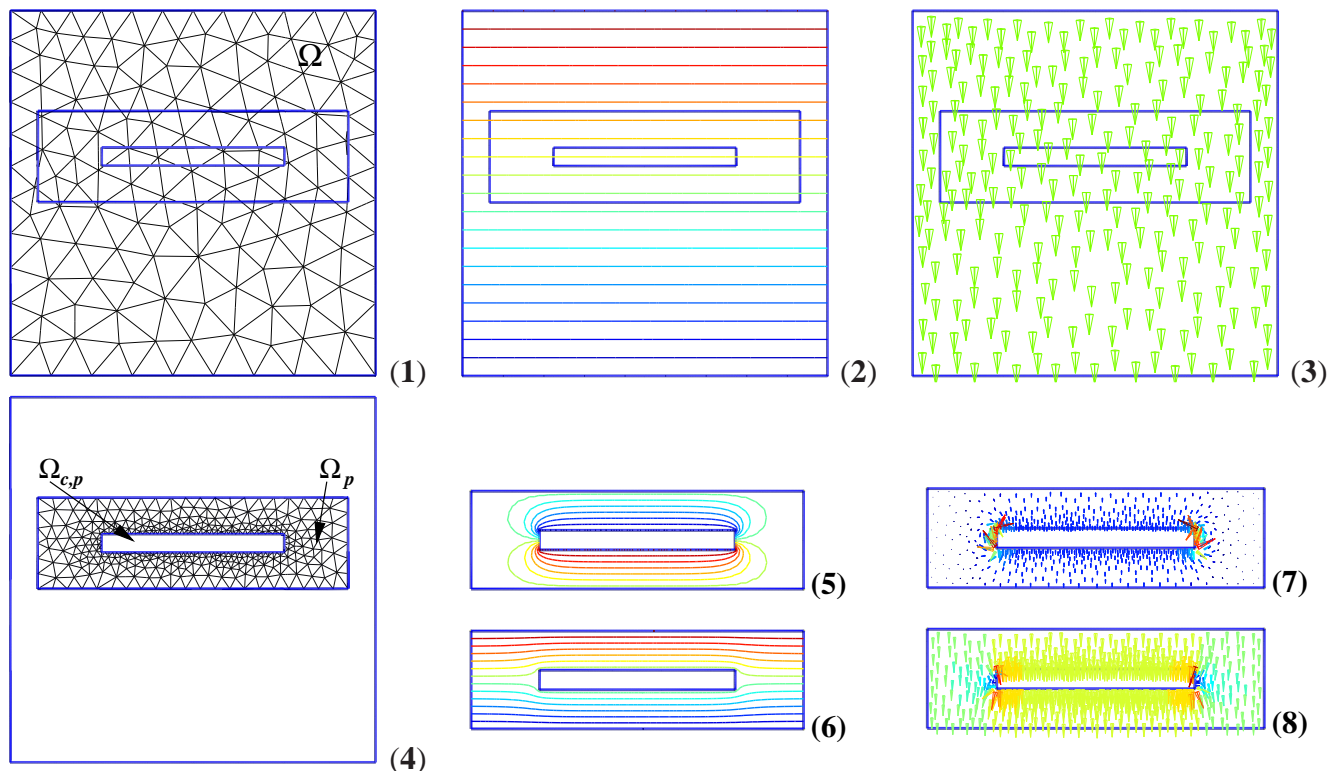


Figure 2. Mesh of Ω (1); distribution of the unperturbed electric potential v_u (2) and electric field e_u (3); adapted mesh of Ω_p (4); distribution of the perturbation electric potential v (5) and the perturbed one v_p (6); distribution of the perturbation electric field e (7) and the perturbed one e_p (8)

For each iteration i ($i = 0, 1, \dots$), we determine the electric scalar potential v_{2i} in Ω , with $v_0 = v_u$. The projection of this solution from its original mesh to that of the added conductor $\Omega_{c,p}$ gives a source $v_{s,2i+1}$ for a perturbation problem. This way, we obtain a potential v_{2i+1} in $\partial\Omega_{c,p}$ that will counterbalance the potential in $\partial\Omega_c$. A new source $v_{s,2i+2}$ for the initial configuration has then to be calculated. This is done by projecting v_{2i+1} from its support mesh to that of Ω as follows

$$(\mathbf{grad} v_{s,2i+2}, \mathbf{grad} v')_{\partial\Omega_c} - (\mathbf{grad} v_{2i+1}, \mathbf{grad} v')_{\partial\Omega_c} = 0, \quad \forall v' \in F(\partial\Omega_c). \quad (11)$$

A new perturbation electric scalar potential problem is defined in Ω as

$$(-\varepsilon \mathbf{grad} v_{2i+2}, \mathbf{grad} v')_{\Omega} - \langle \mathbf{n} \cdot \mathbf{d}_{2i+2}, v' \rangle_{\Gamma_d} = 0, \quad \forall v' \in F(\Omega), \quad (12)$$

with Dirichlet BC $v_{2i+2} = -v_{s,2i+2} |_{\partial\Omega_c}$.

This iterative process is repeated until convergence for a given tolerance.

5. Application

A parallel-plate capacitor (Fig. 1) is considered as a 2-D FE test case to illustrate and validate the perturbation method for electrostatic field distortions (length of plates = $200 \mu\text{m}$, distance between plates: $d = 200 \mu\text{m}$). The conducting parts Ω_c of the capacitor are two electrodes between which the difference of electric potential is $\Delta V = 1\text{V}$ (upper electrode fixed to 1V). The perturbing conductive region $\Omega_{c,p}$ is

a micro-beam (length= $100 \mu\text{m}$, width= $10 \mu\text{m}$). This perturbing region is placed at a distance d_1 of the electrode at 1V.

First, we study the accuracy of the perturbation method as a function of the size of the perturbing domain. In this case, $d_1 = 75 \mu\text{m}$. Fig. 3 shows examples of meshes for the perturbing problems. An adapted mesh, specially fine in the vicinity of the corners of the micro-beam is used. Note that any intersection of perturbation problem boundaries with the unperturbed problem material regions is allowed.

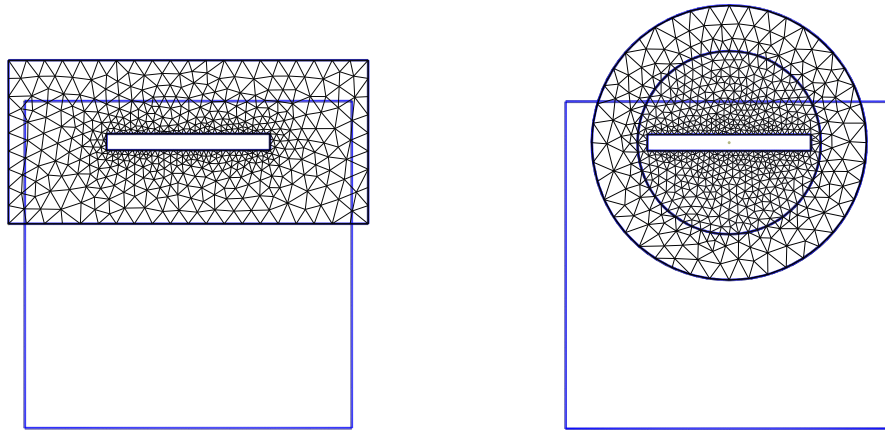


Figure 3. Meshes for the perturbation problems without (*left*) and with a shell for transformation to infinity (*right*)

The electrostatic field between the plates of the capacitor is first calculated in the absence of the micro-beam. The solution of this problem is then evaluated on the added micro-beam and used as a source for the so-called perturbation problem.

In Fig. 4(*left*), the local electric field is depicted for different sizes of the perturbation domain. The first one is a rectangular bounded perturbation region (length= $170 \mu\text{m}$, width= $50 \mu\text{m}$). The second one is a rectangular perturbation domain as well (length= $180 \mu\text{m}$, width= $150 \mu\text{m}$). The third one is an extended perturbation region to infinity through a shell transformation [15].

Comparing with the conventional FE solution, we observe that the relative error of the local electric field is under 1.2% when the perturbation domain is extended to infinity through a shell transformation (Fig. 4(*right*)). This justifies our choice for this kind of perturbation region for the whole of our study.

The relative error of the electric potential and the electric field near the micro-beam increases when the latter is close to electrode at 1V (Fig. 5) what highlights a significant coupling of these regions. A more accurate solution for close positions needs an iterative process to calculate successive perturbations in each region.

To illustrate the iterative perturbation process, the distance $d_1 = 3 \mu\text{m}$ is chosen as an example (Fig. 6). Successive perturbation problems defined in each region are solved.

At iteration 0, the unperturbed electric potential scalar is computed in the whole domain Ω . Projecting this quantity in the domain Ω_p at iteration 1 leads to a perturbed electric potential scalar v_p ensuing the electric field perturbation e_p . The relative error of the electric scalar potential computed near the micro-

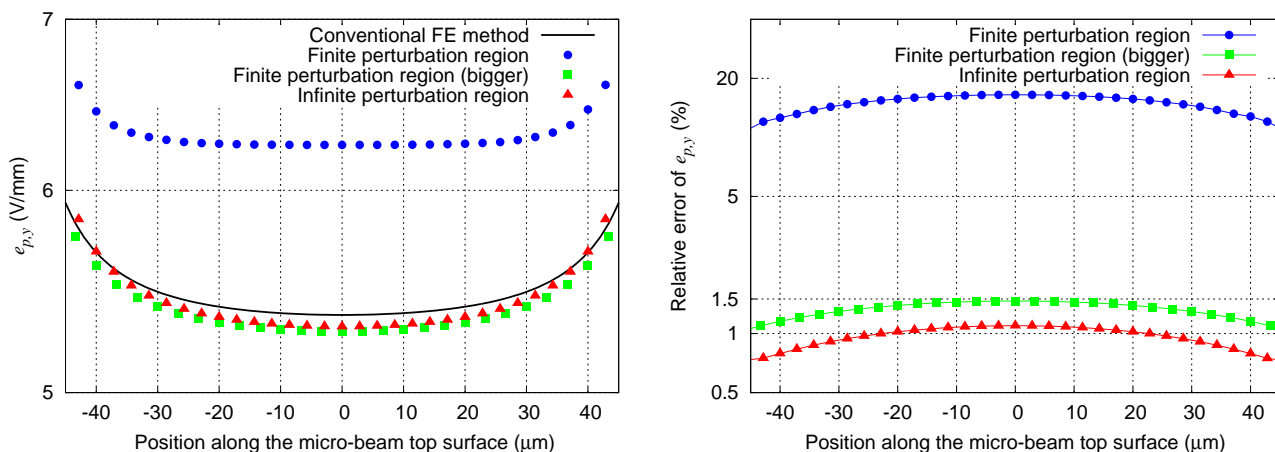


Figure 4. e_p (y -component) computed along the micro-beam top surface for different perturbing regions (left). Relative error of e_p (y -component) with respect to the FE solution in each perturbing region (right)

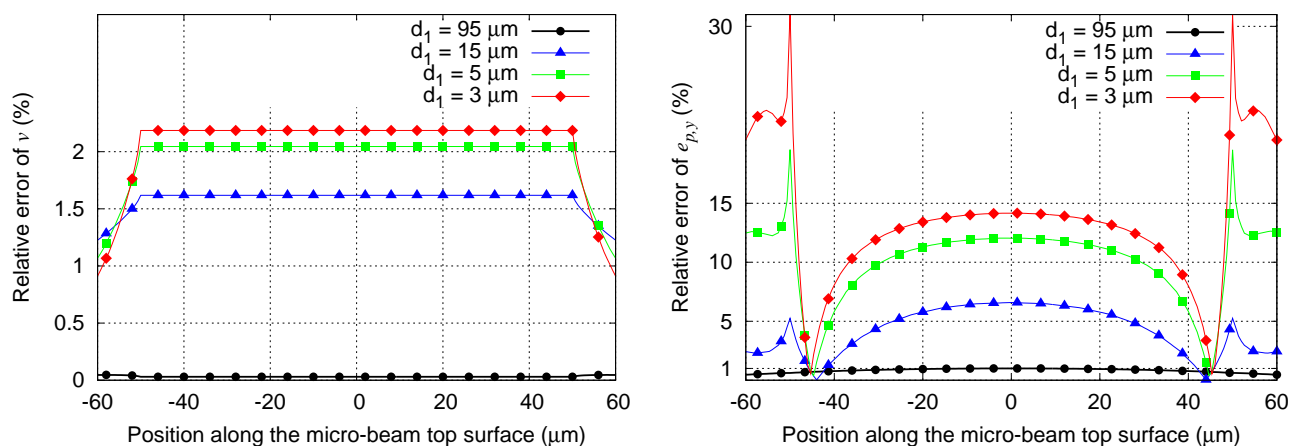


Figure 5. Relative error of v_p (left) and e_p (y -component) (right) computed along the micro-beam top surface for several distances separating electrode at 1V and the micro-beam

beam with respect to the conventional FE technique is bigger than 2% (Fig. 6 (left)). Besides, the difference between the y -components of e_p and the reference solution (FE) is considerable (relative error up to 32%) which is due to a strong coupling between these regions (Fig. 6 (right)). At iteration 2, v is projected from its mesh to that of Ω where a new perturbation problem is solved and its solution is projected again in Ω_p (at iteration 3). The relative error of the local electric field at iteration 25 is reduced to 1%.

In order to highlight the relationship between the distance separating the micro-beam and electrode at 1V and the number of iterations required to achieve the convergence without and with Aitken acceleration [16], several positions d_1 of the micro-device are considered (Fig. 7). For each of them, the perturbation problem is solved and an iterative process is carried out till the relative error of the local electric field is smaller than 1%.

As expected, several iterations are needed to obtain an accurate solution when the micro-beam is close

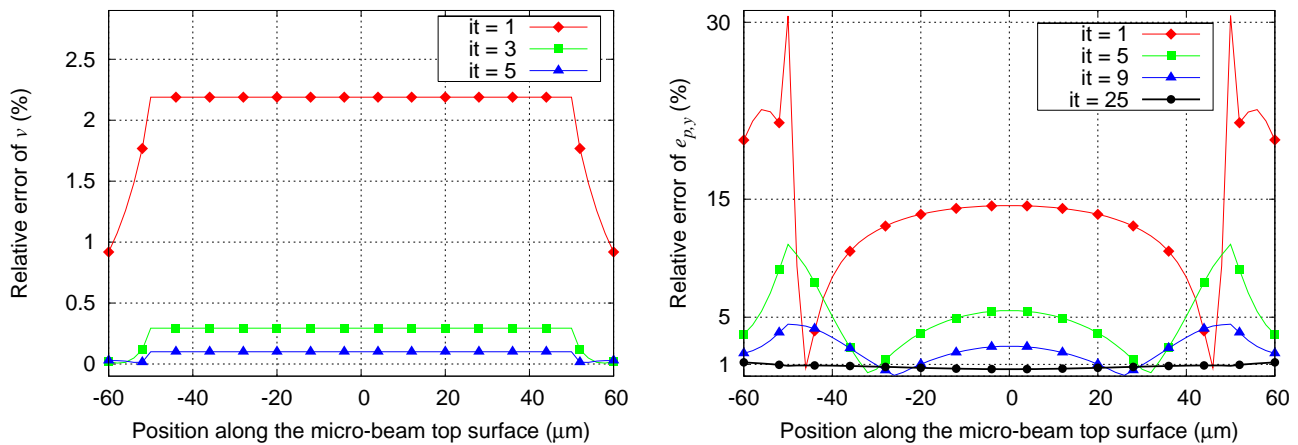


Figure 6. Relative error of v_p (left) and e_p (y-component) (right) computed along the micro-beam top surface for some iterations

to the considered electrode. When the Aitken acceleration is used, the number of iterations is reduced.

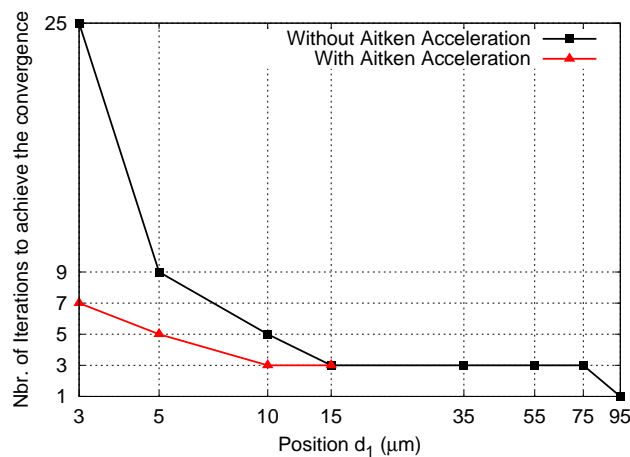


Figure 7. Iteration numbers to achieve the convergence versus the distance separating electrode at 1V and the micro-beam

6. Conclusion

A perturbation method for computing electrostatic field distortions due to the presence of conductive micro-structure has been presented. First, an unperturbed problem (in the absence of certain conductors) is solved with the conventional FE method in the complete domain. Second, a perturbation problem is solved in a reduced region with an additional conductor using the solution of the unperturbed problem as a source.

In order to illustrate and validate this method, we considered a 2-D FE model of a capacitor and a moving micro-beam. Results are compared to those obtained by the conventional FE method. When

the moving region is close to the electrostatic field source, several iterations are required to obtain an accurate solution. Successive perturbations in each region are thus calculated not only from the original source region to the added conductive perturbing domain, but also from the latter to the former. The Aitken acceleration has been applied to improve the convergence of the iterative process.

Acknowledgements

This work was supported by the Belgian French Community (ARC 03/08-298) and the Belgian Science Policy (IAP P6/21).

References

1. Batra, R. C.; Porfiri, M.; Spinello, D. Review of modeling electrostatically actuated microelectromechanical systems. *Smart Materials and Structures* **2007**, *16*, R23–R31.
2. Younis, M. I.; Abdel-Rahman, E. M.; Nayfeh, A. A reduced-order model for electrically actuated microbeam-based MEMS. *Journal of Microelectromechanical Systems* **2003**, *12*(5), 672–680.
3. Osterberg, P. M.; Senturia, S. D. M-test: A test chip for MEMS material property measurement using electrostatically actuated test structures. *Journal of Microelectromechanical Systems* **1997**, *6*(2), 107–118.
4. Boutaayamou, M.; Nair, K. H.; Sabariego, R. V.; Dular, P. Finite element modeling of electrostatic MEMS including the impact of fringing field effects on forces. *In press in Sensor Letters* **2007**.
5. Zhang, L. X.; Zhao, Y. P. Electromechanical model of RF MEMS switches. *Microsystem Technologies* **2003**, *9*, 420–426.
6. Zhang, L. X.; Yu, T. X.; Zhao, Y. P. Numerical analysis of theoretical model of the RF MEMS switches. *Acta Mechanica Sinica* **2004**, *20*(2), 178–184.
7. Rochus, V.; Rixen, D.; Golinval, J.-C. Modeling of electro-mechanical coupling problem using the finite element formulation. In *Proceedings of the 10th SPIE*, volume 5049, pages 349–360, **2003**.
8. Badics, Z.; Matsumoto, Y.; Aoki, K.; Nakayasu, F.; Uesaka, M.; Miya, K. An effective 3-D finite element scheme for computing electromagnetic field distortions due to defects in eddy-current nondestructive evaluation. *IEEE Transactions on Magnetics* **1997**, *33*(2), 1012–1020.
9. Dular, P.; Sabariego, R. V. A perturbation finite element method for modeling moving conductive and magnetic regions without remeshing. *The international journal for computation and mathematics in electrical and electric engineering* **2007**, *26*(3), 700–711.
10. Dular, P.; Sabariego, R. V. A perturbation finite element method for computing field distortions due to conductive regions with *h*-conform magnetodynamic finite element formulations. *IEEE Transactions on Magnetics* **2007**, *43*(4), 1293–1296.
11. Sebestyen, I. Electric field calculation for HV insulators using domain decomposition method. *IEEE Transactions on Magnetics* **2002**, *38*(2), 1213–1216.
12. Stratton, J. A. *Electromagnetic Theory*. McGraw-Hill, **1941**.
13. Dular, P.; Legros, W.; Nicolet, A. Coupling of local and global quantities in various finite element formulations and its application to electrostatics, magnetostatics and magnetodynamics. *IEEE*

Transactions on Magnetism **1998**, *34*(5), 3078–3081.

14. Geuzaine, C.; Meys, B.; Henrotte, F.; Dular, P.; Legros, W. A Galerkin projection method for mixed finite elements. *IEEE Transactions on Magnetism* **1999**, *35*(3), 1438 – 1441.
15. Brunotte, X.; Meunier, G.; Imhoff, J.-F. Finite element modeling of unbounded problems using transformations: a rigorous, powerful and easy solution. *IEEE Transactions on Magnetism* **1992**, *28*(2), 1663–1666.
16. Weniger, E. J. Prediction properties of Aitken's iterated δ^2 process, of Wynn's epsilon algorithm and of Brezinski's iterated theta algorithm. *Journal of Computational and Applied Mathematics* **2000**, *122*(1-2), 329–356.

© 2008 by MDPI (<http://www.mdpi.org>). Reproduction is permitted for noncommercial purposes.